

positive constant. Thus, the magnitude of λ_H is governed by two opposing factors: One factor increases λ_H linearly with increasing n_H (that is, $\lambda_H \propto n_H$) while the other factor decreases λ_H linearly with increasing n_H (that is, $\lambda_H \propto C - n_H$). It is important to note that the λ_H versus n_H plot has the shape of an inverted parabola (with the maximum at $n_H = C/2$). This character of λ_H is ultimately responsible for the inverted parabolic shape observed for the T_c versus n_H plots. It is crucial to understand the exact origin of the $\lambda_H \propto n_H (C - n_H)$ relationship. As plausible reasons, we suggest the following: Cooper pair formation is enhanced with shortening the average distance between holes and thus with increasing n_H , which might lead to the $\lambda_H \propto n_H$ relation. Certain physical parameters associated with the in-plane Cu-O bond (for example, the in-plane Cu-O bond polarizability and the softness of the in-plane Cu-O bond stretching or bending vibration) decrease their magnitudes with increasing n_H . If such physical parameters are responsible for Cooper pair formation, the $\lambda_H \propto C - n_H$ relation might result. Then, combination of the two opposing effects would lead to the relationship $\lambda_H \propto n_H(C - n_H)$, which is a necessary condition that any satisfactory pairing mechanism must accommodate. Note that λ consists of an n_H -dependent term, λ_H , and an n_H -independent term, λ_0 . It is possible that λ_0 originates from the electron-phonon coupling mechanism and λ_H from a new pairing mechanism yet to be determined.

REFERENCES AND NOTES

- M. W. Shafer, T. Penney, B. L. Olsen, *Phys. Rev. B* **36**, 4047 (1987).
- J. B. Torrance, *et al.*, *Phys. Rev. Lett.* **61**, 1127 (1988).
- W. A. Groen, D. M. de Leeuw, L. F. Feiner, *Physica C* **165**, 55 (1990).
- W. A. Groen, D. M. de Leeuw, G. P. J. Geelen, *ibid.*, p. 305.
- T. Penney, M. W. Shafer, B. L. Olsen, *ibid.* **162-164**, 63 (1989).
- M. W. Shafer, T. Penney, B. L. Olsen, R. L. Greene, R. H. Koch, *Phys. Rev. B* **39**, 2914 (1989).
- D. B. Mitzi *et al.*, *ibid.* **38**, 6667 (1988).
- R. Liang, M. Itoh, T. Nakamura, *Physica C* **157**, 83 (1989).
- Y. Tokura, J. B. Torrance, T. C. Huang, A. I. Nazzari, *Phys. Rev. B* **38**, 7156 (1988).
- Y. Ohta, T. Tohyama, S. Maekawa, *Physica C* **166**, 385 (1990).
- J. B. Torrance and R. M. Metzger, *Phys. Rev. Lett.* **63**, 1515 (1989).
- R. Asokamani and R. Manjula, *Phys. Rev. B* **39**, 4217 (1989).
- S. Balasubramanian and K. J. Rao, *Solid State Commun.* **71**, 979 (1989).
- J. Gopalakrishnan, M. A. Subramanian, A. W. Sleight, *J. Solid State Chem.* **80**, 156 (1989).
- D. A. Nepela and J. M. McKay, *Physica C* **158**, 65 (1989).
- M.-H. Whangbo *et al.*, *ibid.*, p. 371.
- C. C. Torardi, D. Jung, D. B. Kang, J. Ren, M.-H. Whangbo, *Mat. Res. Soc. Symp. Proc.* **156**, 295 (1989).
- R. S. Markiewicz and B. G. Giessen, *Physica C* **160**, 497 (1989).

- R. J. Cava, *et al.*, *ibid.* **165**, 419 (1990).
- I. D. Brown, *J. Solid State Chem.* **82**, 122 (1989), and references therein.
- J. L. Tallon and G. V. M. Williams, paper (A-V.3) presented at the meeting of the European Materials Research Society, Strasbourg, France, 29 May to 1 June 1990.
- D. M. de Leeuw, W. A. Groen, L. F. Feiner, E. E. Havinga, *Physica C* **166**, 133 (1990).
- J. B. Parise and E. M. McCarron, paper presented at the Materials Research Society Symposium, Boston, 27 November to 2 December 1989.
- Y. J. Uemura *et al.*, *Phys. Rev. Lett.* **62**, 2317 (1989).
- M.-H. Whangbo, M. Evain, M. A. Beno, J. M. Williams, *Inorg. Chem.* **26**, 1829 (1987).
- M.-H. Whangbo, M. Evain, M. A. Beno, J. M. Williams, in *High-Temperature Superconducting Materials: Synthesis, Properties and Processing*, W. E. Hatfield and J. H. Miller, Jr., Eds. (Dekker, New York, 1988), p. 181.
- I. D. Brown and R. D. Shannon, *Acta Crystallogr. A* **29**, 266 (1973).
- I. D. Brown and D. Altermatt, *Acta Crystallogr. B* **41**, 244 (1985).
- Calculated on the basis of the crystal structures reported by Weiss and Faivre (40). The r_0 value of the Sn-O bond is 1.905 Å (28).
- J. M. Tarascon, L. H. Greene, W. R. McKinnon, G. W. Hull, T. H. Geballe, *Science* **235**, 1373 (1987).
- Y. Le Page, W. R. McKinnon, J.-M. Tarascon, P. Barbois, *Phys. Rev. B* **40**, 6810 (1989), and references therein.
- W. A. Groen and D. M. de Leeuw, *Physica C* **159**, 417 (1989).
- Y. T. Huang, R. S. Liu, W. N. Wang, P. T. Wu, *Jpn. J. Appl. Phys.* **28**, L1514 (1989).
- J. D. Jorgensen *et al.*, *Phys. Rev. B* **36**, 3608 (1987).
- J. D. Axe *et al.*, *Phys. Rev. Lett.* **62**, 2751 (1989); A. R. Moodenbaugh, Y. Xu, M. Suenaga, T. J. Fokerts, R. N. Shelton, *Phys. Rev. B* **38**, 4596 (1988).
- J. Bardeen, L. N. Cooper, J. R. Schrieffer, *Phys. Rev.* **108**, 1175 (1957).
- W. L. McMillan, *ibid.* **167**, 331 (1968).
- K. H. Bennemann, *Solid State Commun.* **67**, 431 (1988).
- J. Ruvalds, *Phys. Rev. B* **35**, 8869 (1987).
- R. Weiss and R. Faivre, *Comptes Rendus. Heb. Seanc. Acad. Sci.* **248**, 106 (1959).
- J. B. Parise, N. Herron, M. K. Crawford, P. L. Gai, *Physica C* **159**, 255 (1989).
- Structural figures were drawn with the assistance of the ORTEP program, written by C. K. Johnson, 1976.
- We thank J. Cameron and J. J. Novoa for their help in the error analysis. Work at North Carolina State University is supported by the Office of Basic Energy Sciences, Division of Materials Sciences, U.S. Department of Energy under grant DE-FG05-86ER45259.

25 June 1990; accepted 25 July 1990

Thin Films of *n*-Si/Poly-(CH₃)₃Si-Cyclooctatetraene: Conducting-Polymer Solar Cells and Layered Structures

MICHAEL J. SAILOR, ERIC J. GINSBURG, CHRISTOPHER B. GORMAN, AMIT KUMAR, ROBERT H. GRUBBS,* NATHAN S. LEWIS*

The optical and electronic properties of thin films of the solution-processible polymer poly-(CH₃)₃Si-cyclooctatetraene are presented. This conjugated polymer is based on a polyacetylene backbone with (CH₃)₃Si side groups. Thin transparent films have been cast onto *n*-doped silicon (*n*-Si) substrates and doped with iodine to form surface-barrier solar cells. The devices produce photovoltages that are at the theoretical limit and that are much greater than can be obtained from *n*-Si contacts with conventional metals. Two methods for forming layered polymeric materials, one involving the spin-coating of preformed polymers and the other comprising the sequential polymerization of different monomers, are also described. An organic polymer analog of a metal/insulator/metal capacitor has been constructed with the latter method.

ELECTRONICALLY CONDUCTIVE POLYMERS are currently of interest for their possible applications in electronics (1), nonlinear optics (2), and solar energy conversion systems (3). To date, most synthetic routes to these polymers have produced insoluble, intractable materials with fibrillar or porous morphologies. Consequently, the conventional synthetic routes to conducting organic polymers have precluded the fabrication of uniform, well-

defined electronic or optical structures. Recently, ring-opening metathesis polymerization (ROMP) has allowed the preparation of soluble, processible, conductive polyacetylenes (4, 5). In this work we demonstrate that this new synthetic route can be exploited to fabricate thin films of conducting organic polymers for possible use in several electronic and optical applications. These include semiconductor/organic polymer junctions for solar cells and layered polymeric structures for potential use as polymer-based capacitors or optical waveguides.

Our synthetic procedure utilized the tungsten carbene complex W(CHC(CH₃)₃) (N-2,6-(CH(CH₃)₂)₂-C₆H₃) (OC(CH₃)(CF₃)₂)₂ (6) to catalyze the ROMP route with substituted cyclooctatetraenes (COT),

Arnold and Mabel Beckman Laboratory of Chemical Synthesis and the Arthur A. Noves Laboratory of Chemical Physics, The Division of Chemistry and Chemical Engineering, California Institute of Technology, Pasadena, CA 91125.

*To whom correspondence should be addressed.

yielding substituted polyacetylenes (4, 5). The polymer substituents lend solubility and processibility to the materials while allowing a reasonably high conductivity in the doped films. For example, polymerization of $(\text{CH}_3)_3\text{Si}$ -cyclooctatetraene typically produced substituted polyacetylene films of 10^4 molecular weight (by gel permeation chromatography versus polystyrene) that were soluble in tetrahydrofuran (THF). The polymer was then photochemically converted into the trans configuration (4), and the THF solutions were cast into thin films by using conventional spin coating procedures.

Scanning electron microscope (SEM) images are shown in Fig. 1 of polymer films that were obtained from conventional polymerization of acetylene (7) (Fig. 1A), from the ROMP route with unsubstituted COT (Fig. 1B), and from the spin-coating of soluble poly- $(\text{CH}_3)_3\text{Si}$ -COT (Fig. 1C). These images demonstrate the greater homogeneity of the recast poly- $(\text{CH}_3)_3\text{Si}$ -COT films with respect to the as-polymerized films. The gas phase polymerization of acetylene (Shirakawa polyacetylene) results in a spongy material with fibrils that are apparent at $\times 8000$ magnification (8, 9). At the same magnification, an as-polymerized film of poly-COT also displays a roughly textured surface, although it is smoother than the Shirakawa sample. The recast poly- $(\text{CH}_3)_3\text{Si}$ -COT sample, by comparison, is much smoother and displays no discernible features up to the limit of resolution of the SEM (~ 200 nm). For the purpose of making the solar cells and layered polymeric structures described below, the homogeneity of recast poly- $(\text{CH}_3)_3\text{Si}$ -COT ensures that the morphology of the solid-polymer interface is uniform.

As with unsubstituted polyacetylene, poly- $(\text{CH}_3)_3\text{Si}$ -COT is a poor conductor (resistivity $> 6 \times 10^5 \Omega\text{-cm}$) until it is doped with a chemical oxidant (9). On exposure to iodine vapor the resistivity of poly- $(\text{CH}_3)_3\text{Si}$ -COT films decreased to between 0.2 to 1 $\Omega\text{-cm}$, as measured by standard four-point probe techniques. The broad absorption in the visible spectrum associated with the undoped polymer ($\lambda_{\text{max}} = 538$ nm; absorption coefficient $\alpha = 10^5 \text{ cm}^{-1}$) disappeared on exposure of the film to iodine vapor; the absorption spectrum of the resulting doped film was fairly featureless in the visible region, with α values ranging from 3×10^4 to $6 \times 10^4 \text{ cm}^{-1}$. For a comparable absorption (at $\lambda = 520$ nm), the sheet resistance R_s of a poly- $(\text{CH}_3)_3\text{Si}$ -COT film is about three orders of magnitude greater than that of a gold metal film ($R_s = 6 \times 10^4 \Omega/\text{square}$ for a 440 \AA poly- $(\text{CH}_3)_3\text{Si}$ -COT film; $R_s = 10$

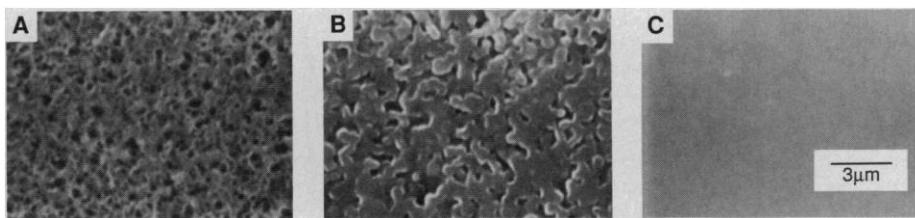


Fig. 1. Scanning electron microscope images (15-keV secondary electron images at the same magnification) of: (A) polyacetylene produced by polymerization of acetylene gas (Shirakawa polyacetylene); (B) poly-cyclooctatetraene (poly-COT) produced by the liquid-phase ROMP route with COT; and (C) poly- $(\text{CH}_3)_3\text{Si}$ -COT that has been recast from THF solution. All samples were doped to metallic conductivity with $\text{I}_2(\text{g})$ and imaged without metal coating.

Ω/square for a 100 \AA Au film on glass).

We have exploited the ability to form relatively transparent, uniform layers of these conducting polymers in the formation of n -Si/polyacetylene junctions that act as solar cells. The current-voltage properties of an n -Si/poly- $(\text{CH}_3)_3\text{Si}$ -COT interface and an n -Si/Au contact (tungsten-halogen illumination, filtered through a 9-cm water column) are compared in Fig. 2. From Fig. 2 it is apparent that under comparable short circuit current densities the polymer-based cell produces a much higher open-circuit voltage, V_{oc} , than the conventional metal contact. Interfaces between inorganic metals and n -Si exhibit poor photovoltaic behavior because chemical reactions at the Si/metal boundary lead to high recombination rates that are independent of the metal used (10). This non ideal behavior results in low open circuit voltages and low solar conversion efficiencies for n -Si/metal cells. In contrast, the I_2 -doped poly- $(\text{CH}_3)_3\text{Si}$ -COT makes a contact with n -Si that produces larger open circuit voltages than can be obtained with conventional metal Schottky barriers. Fur-

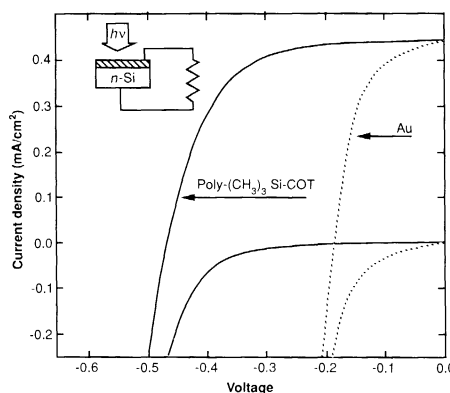


Fig. 2. Current density versus voltage curves for poly- $(\text{CH}_3)_3\text{Si}$ -COT/ n -Si (solid line) and Au/ n -Si (dashed line) solar cells in the dark and under illumination (n -Si resistivity is 3.2 $\Omega\text{-cm}$). Note that at comparable current densities the conventional Au/ n -Si device produced a significantly lower photovoltage than the polymer-based device. The light intensity on the poly- $(\text{CH}_3)_3\text{Si}$ -COT/ n -Si cell was 9 mW/cm^2 (tungsten-halogen lamp), and the conversion efficiency was 1.5%.

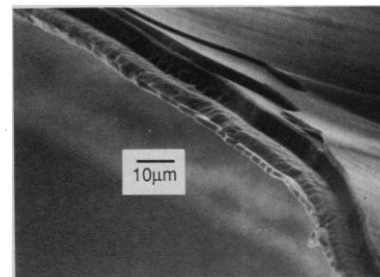


Fig. 3. Scanning electron microscope image (20-keV backscattered electron image) of a layered structure produced by successive casting and $\text{I}_2(\text{g})$ doping of poly- $(\text{CH}_3)_3\text{Si}$ -COT and poly- $(\text{CH}_3)_3\text{Sn}$ -COT solutions. The sandwich structure was freeze-fractured and is viewed in cross section.

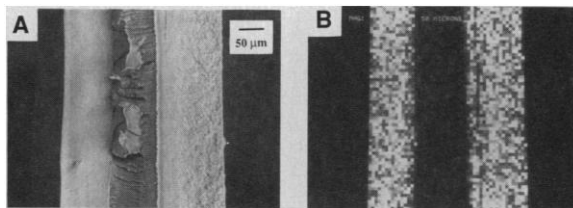
thermore, the photovoltages measured on the poly- $(\text{CH}_3)_3\text{Si}$ -COT/ n -Si devices are at the maximum allowed for surface barrier devices.

When interfacial recombination is made negligibly small, the upper limit on V_{oc} is determined by carrier recombination in the bulk of the Si. The theoretical maximum V_{oc} , based on this bulk diffusion-recombination process, is given by Eq. 1:

$$V_{\text{oc}} = (kT/q) \ln [J_{\text{ph}} L_{\text{p}} N_{\text{D}} / q D_{\text{p}} n_i^2] \quad (1)$$

where k is the Boltzmann constant, T the temperature, q the electronic charge, and J_{ph} is the photocurrent density. The other terms are properties of the particular Si sample used: L_{p} is the hole diffusion length, N_{D} is the number density of dopant atoms, D_{p} is the hole diffusion coefficient, and n_i is the intrinsic carrier concentration (11, 12). Table 1 lists the V_{oc} values obtained on a series of n -Si/poly- $(\text{CH}_3)_3\text{Si}$ -COT cells constructed from Si of different resistivities (dopant densities) and diffusion lengths. Also presented are V_{oc} values for the corresponding n -Si/Au contacts and values of V_{oc} calculated from Eq. 1. The polymer-based cells studied in this work all reached the bulk recombination limit, indicating that there were negligible losses due to charge-carrier trapping at the Si/polymer interface. Thus the Si/polymer junction is superior to conventional Si/metal junctions, whose V_{oc} val-

Fig. 4. (A) Scanning electron microscope image (20-keV backscattered electron image) of a polyacetylene/polybutadiene/polyacetylene "capacitor" structure in cross section. (B) Iodine element map of the same structure, showing the presence of the iodine dopant in the polyacetylene layers. The iodine dopant renders the polyacetylene layers metallically conductive in this conductor/insulator/conductor sandwich.



ues are limited to 200 to 300 mV by interfacial Fermi-level pinning (10). The polymer system also compares favorably with Si *p-n* junction solar cells, which typically display V_{oc} values below the theoretical limit (13). The unoptimized *n*-Si/poly-(CH₃)₃Si-COT devices showed overall solar conversion efficiencies of between 1 and 5% under high light intensities (80 to 100 mW/cm²), with the main sources of efficiency loss being series and parallel (shunting) resistances [electrical contacts to the polymer were made with Au wires or with transparent indium tin oxide (ITO)-coated glass slides; typically $R_s = 100 \Omega$ and $R_p = 10^5 \Omega$ for the ITO contacts]. The efficiencies also were not corrected for reflection or absorption losses, which could be minimized to increase the incident-light-based quantum yield [the $\sim 200 \text{ \AA}$ thick poly-(CH₃)₃Si-COT layer transmits between 89 to 94% of the light in the visible region].

The ability to process these polymers can also be exploited to fabricate multilayer structures. We have prepared electrically conductive laminar structures of the soluble conjugated polymers poly-(CH₃)₃Si-COT and poly-(CH₃)₃Sn-COT (trimethylstannylcyclooctatetraene) by taking advantage of the insolubility of I₂-doped poly-(CH₃)₃Si-COT and poly-(CH₃)₃Sn-COT in THF. A layer of poly-(CH₃)₃Si-COT was cast from THF solution, and the resulting film was doped with I₂ in an evacuated chamber. A layer of poly-(CH₃)₃Sn-COT was then cast on top of the Si-containing polymer with no noticeable dissolution of the underlying doped poly-(CH₃)₃Si-COT film. After exposure of the structure to the iodine dopant, a third layer, consisting of poly-(CH₃)₃Si-COT, was cast and then I₂-doped. The process could be continued indefinitely. In Fig. 3 an SEM image is shown in cross section of a five-layer sandwich made in this fashion. The sharp boundary observed between the layers is an indication of the segregation of the Si- and Sn-containing polymers. The layers shown in Fig. 3 were deliberately made thick enough to facilitate imaging in the SEM; sandwich structures with 1000 \AA layers have been resolved in the SEM, and single layers with thicknesses of

100 \AA (as determined by profilometry) have also been produced by spin-coating techniques. Thin multilayered structures are of interest for their potential use as waveguides and electrooptic modulators (14).

We have also used the ROMP procedure to make multilayers of either conducting or insulating polymer films. The tungsten carbene catalyst has been found to polymerize cyclooctadiene (COD) to yield nonconjugated (and electrically insulating) polybutadiene (15), and this implies that the ROMP route can be used to prepare layers of conductors in contact with layers of insulators. To demonstrate this possibility, a polyacetylene/polybutadiene/polyacetylene "sandwich" was fabricated by pouring the monomer COD onto an already polymerized COT layer. The active catalyst residues remaining in the poly-COT layer were sufficient to polymerize the added COD. An additional aliquot of COT was then deposited onto the resultant poly-COD (polybutadiene) layer, and the COT subsequently polymerized, resulting in the completed "sandwich" structure. On exposure of the "sandwich" to I₂(g) followed by removal of excess I₂ in vacuo, a polymeric capacitor was obtained. The SEM image of a freeze-fractured cross section of one of these structures is shown in Fig. 4, along with an iodine element map (from an x-ray emission image at the iodine L _{α} energy). As expected from bulk properties, the iodine preferentially doped into the polyacetylene layers. A typical capacitance was $3.4 \pm 0.1 \text{ pF}$ (measured at a frequency of 1.0 MHz) for a sample with a parallel plate area of 19 mm² and a polybutadiene thickness ranging from 25 to 100 μm . These capacitor structures demonstrate the versatility of the ROMP technique in the fabrication of electronic structures. Of course, fabrication of a practical device would require attention to factors such as pinholes, current leakage, and series resistance of the thin polymer films, which have not been addressed in this chemical synthesis study.

The recent introduction of convenient routes into processible electronically conductive polymers has led to an increased interest in these materials (16). In this work, the ability to form well-defined, reproduc-

Table 1. Open circuit voltages at 20 mA/cm² short circuit current density and 296 K for poly-(CH₃)₃Si-COT/*n*-Si and Au/*n*-Si solar cells. Theory values are the maximum possible V_{oc} calculated from Eq. 1. Diffusion lengths were measured by spectral response; when the apparent L_p obtained from this method was greater than one-half the wafer thickness, the total wafer thickness was used for L_p (11). Values of V_{oc} are averages based on two to five samples, with the sample-to-sample (of the same Si resistivity) variation of less than 5 mV.

<i>n</i> -Si resistivity ($\Omega\text{-cm}$)	L_p (μm)	V_{oc} (V)		
		Theory	Polymer/Si	Au/Si
0.245	315	0.64	0.64	0.30
1.0	337	0.59	0.59	0.28
1.59	13	0.50	0.49	0.30
3.54	382	0.56	0.57	0.29
12.4	387	0.53	0.53	0.30

ible interfaces with poly-(CH₃)₃Si-COT and Si substrates facilitated the systematic study of the properties of these junctions. Conducting polymer/semiconductor solar cells have previously been fabricated by other routes (17-19), and it is clear that some configurations (for instance, polythiophene electropolymerized onto GaAs) can have high solar conversion efficiencies (18). In the present work, the observation of the control of V_{oc} solely by the quality of the Si used shows that the problems inherent to Si/metal interfaces can be overcome at Si/conducting polymer interfaces. Although this is an exciting result from a fundamental viewpoint, practical applications of these films would have to deal with the limited air stability of unprotected poly-(CH₃)₃Si-COT, which shows almost total loss of conductivity after a few days in air. In this respect, the more stable doped polythiophenes are also attractive candidates for study in thin-film form. The versatility of the ROMP procedure and the processibility of some of the resulting polymers synthesized in this work have expedited the fabrication of laminar structures, which is an important step in the potential fabrication of organic waveguides or other electronic devices. The electronic properties and processibility of these materials should lead to additional applications in these areas.

REFERENCES AND NOTES

1. J. H. Burroughes, C. A. Jones, R. H. Friend, *Nature* **335**, 137 (1988).
2. S. R. Marder, J. W. Perry, F. L. Klavetter, R. H. Grubbs, *Chem. Mater.* **1**, 171 (1989), and references cited therein.
3. F. Garnier and G. Horowitz, *Makromol. Chem. Macromol. Symp.* **8**, 159 (1987); J. Kanicki, in *Handbook on Conjugated Electrically Conducting Polymers*, T. A. Skotheim, Ed. (Dekker, New York, 1986), pp. 609-613; A. V. Vannikov and T. S. Zhuravleva, *J. Mol. Electron.* **5**, 63 (1989).

4. E. J. Ginsburg, C. B. Gorman, S. R. Marder, R. H. Grubbs, *J. Am. Chem. Soc.* **111**, 7621 (1989).
5. C. B. Gorman, E. J. Ginsburg, S. R. Marder, R. H. Grubbs, *Angew. Chem. Adv. Mater.* **101**, 1603 (1989).
6. C. Schaverien, J. Dewan, R. R. Schrock, *J. Am. Chem. Soc.* **108**, 2771 (1986).
7. A. M. Saxman, R. Liepins, M. Aldissi, *Prog. Polym. Sci.* **11**, 57 (1985).
8. M. Aldissi, *Inherently Conducting Polymers: Processing, Fabrication, Applications, Limitations* (Noyes Data, Park Ridge, NJ, 1989).
9. H. Shirakawa, E. J. Louis, A. G. MacDiarmid, C. K. Chiang, A. J. Heeger, *J. Chem. Soc. Chem. Commun.* **1977**, 578 (1977).
10. R. Z. Bachrach, in *Metal-Semiconductor Schottky Barrier Junctions and Their Applications*, B. L. Sharma, Ed. (Plenum, New York, 1984), pp. 93–99; S. M. Sze, *Physics of Semiconductor Devices* (Wiley, New York, 1981), pp. 245–311.
11. N. S. Lewis, *J. Electrochem. Soc.* **131**, 2496 (1984).
12. A. L. Fahrnbruch and R. H. Bube, *Fundamentals of Solar Cells* (Academic Press, New York, 1983), chap. 6.
13. ———, *ibid.*, chap. 7.
14. D. B. Neal *et al.*, *Synth. Met.* **28**, D711 (1989); M. C. J. Young, R. H. Tredgold, P. Hodge, *R. Soc. Chem. Spec. Publ.* **69**, 354 (1989); R. H. Tredgold, M. C. J. Young, P. Hodge, E. Khoshdel, *Thin Solid Films* **151**, 441 (1987).
15. F. L. Klavetter and R. H. Grubbs, *Synth. Met.* **28**, D105 (1989).
16. S. H. Askari, S. D. Rughooputh, F. Wudl, A. J. Heeger, *Polym. Prep.* **30**, 157 (1989); S. Hotta, S. D. V. Rughooputh, A. J. Heeger, F. Wudl, *Macromolecules* **20**, 212 (1987); K. Y. Jen, R. L. Oboodi, R. L. Elsenbaumer, *Polym. Mater. Sci. Eng.* **53**, 79 (1985); K. Y. Jen, M. Maxfield, L. W. Shacklette, R. L. Elsenbaumer, *J. Chem. Soc. Chem. Commun.* **4**, 309 (1987); S. D. V. Rughooputh, M. Nowak, S. Hotta, A. J. Heeger, F. Wudl, *Synth. Met.* **21**, 41 (1987); D. C. Bott *et al.*, *ibid.* **14**, 245 (1986); J. Edwards, W. J. Feast, D. Bott, *Polymer* **25**, 395 (1984).
17. A. J. Frank, S. Glenis, A. J. Nelson, *J. Phys. Chem.* **93**, 3818 (1989); M. Ozaki, D. Peebles, B. R. Weinberger, A. J. Heeger, A. G. MacDiarmid, *J. Appl. Phys.* **51**, 4252 (1980); M. J. Cohen and J. S. Harris, Jr., *Appl. Phys. Lett.* **33**, 812 (1978).
18. F. Garnier and G. Horowitz, *Synth. Met.* **18**, 693 (1987).
19. T. Skotheim, O. Ingnas, J. Prejza, I. Lundstroem, *Mol. Cryst. Liq. Cryst.* **83**, 1361 (1982); T. Skotheim and I. Lundstroem, *J. Electrochem. Soc.* **129**, 894 (1982); T. A. Skotheim and O. Ingnas, *ibid.* **132**, 2116 (1985); G. Nagasubramanian, S. DiStefano, J. Moacanin, in *Polymers for Advanced Technologies: IUPAC International Symposium*, M. Lewin, Ed. (VCH, New York, 1988), pp. 261–268.
20. Supported by NSF grant CHE8814694 and ONR grant N001488K0208. C.B.G. thanks the Jet Propulsion Laboratory, Caltech, for a research fellowship. E.J.G. thanks IBM for a graduate fellowship, and A.K. thanks the Department of Education for a graduate fellowship. Contribution 8134 from the Arnold and Mabel Beckman Laboratory of Chemical Synthesis and the Arthur Amos Noyes Laboratory of Chemical Physics.

7 May 1990; accepted 26 June 1990

Inclusion of Thermal Motion in Crystallographic Structures by Restrained Molecular Dynamics

PIET GROS, WILFRED F. VAN GUNSTEREN, WIM G. J. HOL

A protein crystal structure is usually described by one single structure, which largely omits the dynamical behavior of the molecule. A molecular dynamics method with a time-averaged crystallographic restraint was used to overcome this limitation. This method yields an ensemble of structures in which all possible thermal motions are allowed, that is, in addition to isotropic distributions, anisotropic and anharmonic positional distributions occur as well. In the case of bovine pancreatic phospholipase A₂, this description markedly improves agreement with the observed x-ray diffraction data compared to the results of the classical one-model structure description. Time-averaged crystallographically restrained molecular dynamics reveals large mobilities in the loops involved in lipid bilayer association.

THE CLASSICAL REPRESENTATION OF a protein crystal structure is basically limited to a single site isotropic model for each atom. Because of the limited number of x-ray diffraction data from large biomacromolecules, the thermal parameters of each atom, which describe the fluctuations around the average position, cannot be refined anisotropically. Furthermore, the atomic motions in large proteins may be more complicated and include anharmonicity, as shown in the segmented anisotropic refinement of bovine ribonuclease A (1).

The inability to model anharmonicity and anisotropy gives rise to systematic errors present in the model (2). In molecular dynamics (MD) simulations, the configurational space is explored and thus anisotropic as well as anharmonic distributions of the atoms are obtained as represented by the trajectory of the atoms. However, calculating diffraction data from an unrestrained MD simulation (3) yielded, in the case of bovine pancreatic trypsin inhibitor, a low agreement with the experimental data, that is, a high crystallographic residual R ($= \sum ||\mathbf{F}_o| - |\mathbf{F}_c|| / \sum |\mathbf{F}_o|$, where \mathbf{F}_o and \mathbf{F}_c are the observed and calculated structure factors, respectively) of 0.52.

We have combined MD simulations with

crystallographic data by restraining the structure factor amplitudes taken over the whole ensemble of structures to the observed x-ray data. In this crystallographically restrained MD simulation the following target function is used:

$$E = E_{\text{phys}} + \frac{1}{\sigma_x^2} \sum_s (|\mathbf{F}_o(\mathbf{s})| - k|\mathbf{F}_c(\mathbf{s})|)^2 \quad (1)$$

where E_{phys} represents the bond, bond angle, dihedral, improper dihedral, electrostatic, and Lennard-Jones interaction potentials (4), \mathbf{s} is the reciprocal lattice vector, k is a scale factor, and σ_x is a weighting factor. The essential difference with the MD crystallographic refinement procedure (5, 6) is the use of the ensemble average of calculated structure factors, $\langle \mathbf{F}_c \rangle$, instead of the structure factors of one single structure. We considered similar arguments as Torda *et al.* (7, 8) for combining nuclear magnetic resonance–nuclear Overhauser effect data and MD procedures and used a time-weighted, or “running,” average for the calculation of $\langle \mathbf{F}_c \rangle$ in the restraint:

$$\langle \mathbf{F}_c(\mathbf{s}) \rangle_{t'} = \frac{1}{\tau_x(1 - e^{-t'/\tau_x})} \int_0^{t'} e^{-(t' - t)/\tau_x} \mathbf{F}_c^t(\mathbf{s}) dt \quad (2)$$

where τ_x is the structure factor–memory relaxation time and $\mathbf{F}_c^t(\mathbf{s})$ is a structure factor based on an individual structure at time point t from the trajectory and depends only on positional parameters. No individual thermal parameters are assigned to the atoms. The spread of the atoms as found in the crystal is now represented by the spatial distributions of the atoms in the generated ensemble.

Bovine phospholipase A₂ (BPLA₂) is a 123-residue enzyme that degrades phospholipids and acts primarily on aggregated lipids as in bilayers or in micelles (9). Its crystal structure has been determined at 1.7 Å resolution and refined to a crystallographic residual of 0.171 (10). On the basis of the classic representation of the molecule, with three positional parameters and one thermal parameter per atom, the structure-function relation of phospholipases A₂ has been studied in detail (11–13).

We calculated an ensemble of BPLA₂ structures that was restrained according to Eqs. 1 and 2 to the available x-ray diffraction data. It appeared that crystallographically restrained MD gave a significant better agreement between observed and calculated x-ray data (Fig. 1A) than either conventional x-ray refinement procedure (10) or unrestrained MD (3). The improvement obtained by modeling anisotropy and anharmonicity is most dramatic in the higher resolution shells (Fig. 1A). For instance, for

BIOSON Research Institute, Department of Chemistry, University of Groningen, Nijenborgh 16, 9747 AG Groningen, The Netherlands.